Insights into the interaction between octyl hydroxamic acid and the rutile surface activated by lead ion

Qinbo Cao [1,2], Xiumin Chen [2], Heng Zou [1], Xingcai Yu [1]

[1] Faculty of Land Resources Engineering, Kunming University of Science and Technology, Kunming 650093, Yunnan, PR China

[2] State Key Laboratory of Complex Nonferrous Metal Resources Clean Utilization，Kunming University of Science and Technology，Kunming 650093

Corresponding authors: qinbocao@kust.edu.cn (Qinbo Cao), chenxiumin9@hotmail.com (Xiumin Chen)

Abstract: The flotation of rutile can be enhanced using lead ion as an activator. However, the binding behavior of collector on the activated rutile surface is still not fully understood. In this work, flotation and theoretical calculation approaches were employed to evaluate the activation behavior of lead ion in the flotation of rutile with octyl hydroxamic acid (OHA). Flotation results indicated that the activation flotation with lead ion should be conducted at pH 6.5. The binding features of OHA molecule on the inactivated and Pb-activated rutile surfaces were both investigated by density functional theory (DFT) studies. The OHA molecule may dissociate into OHA⁻ anion on the inactivated rutile surface, generating a new Ti–O bond. Differently, the chelate complex of Pb-OHA anion was generated on the activated rutile surface, producing two Pb–O bonds. The adsorption of OHA onto the activated rutile surface was more stable than that on the inactivated rutile surface, due to the formation of more chemical bonds on the activated rutile surface. The DFT calculation results delineated the role of Pb^{2+} in the rutile flotation with OHA.

Keywords: flotation, rutile, activation, density functional theory, adsorption

1. Introduction

Natural rutile, containing approximately 95% of TiO_2, is an important raw material for the production of titanium metal and titanium pigment (Zhang et al., 2011). The world reserve of rutile is about 62 million metric tons as reported by the United States Geological Survey in 2018 (USGS, 2018). Gravity concentration, electrostatic separation and flotation techniques are widely used for enriching rutile from its deposit. Gravity and electrostatic separation methods are suitable for upgrading rutile in beach sand deposits (Chen et al., 2013; Premaratne and Rowson, 2003). Conversely, flotation is efficient for concentrating rutile, especially for a primary rutile ore (Xiao et al., 2018c).

Several collectors can be employed for rutile flotation, such as oleate, styryl phosphonic acid (SPA), and hydroxamic acids (Liu and Peng, 1999; Wang et al., 2014, 2016; Xiao et al., 2018c). In recent years, some metal ions have been found to be activators for rutile flotation. Bi^{3+} ion has been proved to be an efficient activator for rutile flotation (Xiao et al., 2018a; Xiao et al., 2017). Combined activators of Al^{3+} ions and ethylene diamine tetraacetic acid also enhance the flotation of rutile with SPA at a pH of 2 (Xiao et al., 2018b). Pb-activated rutile can be efficiently floated by amyl xanthate at pH 8 (Yu et al., 2019). When salicylhydroxamic acid was used as a collector, the flotation of rutile can be activated by lead ion at pH 6.5 (Li et al., 2016). This flotation method using lead ion and hydroxamic acid is feasible to be conducted in the industry because no pH modifier is needed to adjust the pH of the slurry.

Although Pb^{2+} has been widely used as an activator for rutile flotation, the adsorption features of hydroxamic acid on the inactivated and Pb-activated rutile surfaces have not been studied in depth. Hydroxamic acid can bind with Ti^{4+} and other metal ions in a solution to form chelation complexes

(Brennan et al., 2016; Yang et al., 2017). However, the Ti atoms on the rutile surface have unique steric features. The (110) surface is the most stable plane of rutile (Perron et al., 2007a), on which a Ti atom bonds to oxygen atoms to form a 5-fold-coordinated (5f) or 6-fold-coordinated Ti (6f) atom (Lu et al., 2010). The chemical environment and steric feature of Ti on the rutile surface are far different from those of Ti^{4+} in solution. Hence, whether or not Ti-hydroxamic acid chelate can be formed on the rutile surface remains unclear.

Previous DFT studies showed that water molecules can adsorb at the Ti sites on the rutile surface; while, some adsorbed molecules may dissociate on the surface (Perron et al., 2007b; Sebbari et al., 2011). It was found that Pb^{2+} may react with rutile surface covered by water molecules to form lead hydroxyl complexes (Zou et al., 2019). The hydration state on the rutile surface is governed by pH. The surface may be covered by water molecules (including dissociated water molecules) in an acidic solution (Perron et al., 2007b) and by OH groups in a basic solution (Předota et al., 2004; Zheng et al., 2016). However, few researchers have addressed the binding behavior of lead species on hydrated rutile surface under an optimal flotation pH value. Moreover, the adsorption structures of hydroxamic acid on the Pb-activated surface has not been studied by DFT calculations.

Currently, our knowledge on the activation flotation of rutile with lead ion and hydroxamic acid is still lacking. Thus, this work aimed to examine the interactions among lead ion, hydroxamic acid and the rutile surface by the results of flotation tests and DFT calculations. Firstly, single-mineral flotation tests were employed to determine the activation behavior of lead ions for rutile flotation with octyl hydroxamic acid (OHA), OH is a prevalent hydroxamic acid for rutile flotation. Moreover, the possible binding models of OHA on the natural and Pb-activated rutile surfaces were probed by DFT calculations, to further understand the activation mechanism of lead ion.

2. Materials and methods

2.1. Minerals and reagents

Rutile pebbles (97% purity) were hand-picked from a rutile deposite belonged to Yunnan Metallurgical Group Co., Ltd. The XRD pattern of the rutile sample was provided in the Fig. S1 in the Supplementary material (Appendix A). OHA (99% purity) was purchased from Sigma-Aldrich Chemicals. Inorganic reagents, including $Pb(NO_3)_2$ (99% purity), HCl (analytically purity grade, 38%) and NaOH (96% purity), were all obtained from Sinopharm Group Co., Ltd.

2.2. Flotation experiments

Single-mineral flotation tests were performed with an XFGC II flotation machine using a 40 mL flotation cell (Jilin Province Ore Exploration Machine Factory, Changchun, China). 2.0 g of rutile sample (−74+45 μm) was used in each test. The rutile sample was conditioned with $Pb(NO_3)_2$ solution (35 mL) in the flotation cell for 3 min, after which a desired amount of OHA solution ($1×10^{-2}$ mol/dm³) was added into the flotation cell. The condition time for OHA was also 3 min. The rutile samples were floated for 2 min using air at a flow rate of 30 cm³/min. Each test was repeated thrice and the average values were reported.

2.3. DFT calculations

DFT calculations were carried out by the Cambridge Sequential Total Energy Package (CASTEP) to investigate the binding models of OHA on the natural and Pb-activated surfaces (Segall et al., 2002). In all calculations, the exchange and correlation potentials were described by the generalized gradient approximation using the PBE functional (Perdew et al., 1996; Perdew and Zunger, 1981). Ultrasoft pseudopotentials were used to treat the interactions between ionic core and valence electrons (Francis and Payne, 1990). A 400 eV kinetic energy cutoff and 3×3×1 k-points mesh were employed for the geometry optimization and energy calculations. The convergence criteria in the calculations were set as (1) an energy tolerance of $1×10^{-6}$ eV/atom, (2) a maximum force tolerance of 0.03 eV/Å and (3) a maximum displacement tolerance of 0.001 Å. Such settings are sufficient to achieve a numerical convergence as determined by the convergence testing.

The adsorption energy (ΔE_{ads}) of OHA or Pb^{2+} on the rutile surface was calculated using the following equation:

$$\Delta E_{ads} = E_{slab+adsorbate} - E_{adsorbate} - E_{slab} \qquad (1)$$

where $E_{adsorbate}$ is the energy of free OHA or Pb^{2+}. $E_{slab+adsorbate}$ and E_{slab} are the energy of the slab model with and without an adsorbate, respectively. In this work, two types slab models of rutile surfaces (11.86×13.13×35.13 Å) were used to represent the hydration state of rutile in water at pH 6.5. The surface models have three Ti-O layers. One rutile surface was covered by water molecules bonded to the 5f-Ti atoms and two water molecules were dissociated on the surface (termed as water-covered surface) (Fig. 1a). Such hydrated surface could occur in water stably (Lu et al., 2010). Another rutile surface was fully covered by OH groups generated by the dissociation of water molecules (termed as OH-covered surface) (Fig. 1b). This surface occurs in a basic solution (Perron et al., 2007b). It is expected that the water-covered and OH-covered rutile surfaces may exist in water at pH 6.5 at a reasonable ratio. The O atoms on the water- and OH-covered rutile surfaces formed 6 sites for the adsorption of Pb^{2+}. These adsorption sites were also noted in Fig. 1 while Fig. S2 illustraes the top view of interactional atoms at each adsorption site. In addition, the energy of Pb^{2+} or OHA in a cubic cell (11.86×13.13×35.13 Å) was calculated with the gamma point.
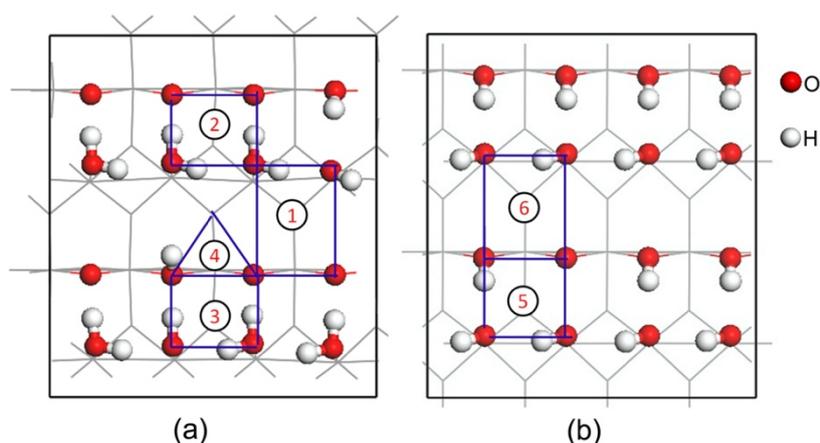

Fig. 1. 4-fold hollow (4FH) sites and 3-fold hollow (3FH) site on the (a) water-covered and (b) OH-covered rutile surfaces allowed for the adsorption of Pb^{2+}: (1) 4FH1 site; (2) 4FH2 site; (3) 4FH3 site; (4) 3FH site; (5) 4FH4 site; (6) 4FH5 site (bottom atoms are shown in a line style to better view the structure)

3.   Results and discussion

3.1. Flotation tests

The pH of the slurry is a vital factor determining the activation behavior of $Pb(NO_3)_2$ in the rutile flotation (Li et al., 2016). Here, the influence of pH on the flotation of rutile with $Pb(NO_3)_2$ and OHA was examined via single-mineral flotation tests. The concentrations of $Pb(NO_3)_2$ and OHA were both 1×10^{-4} mol/dm³ in the tests.

The flotation behavior of natural (inactivated) rutile with OHA was first determined for comparison. As shown in Fig. 2, the recoveries of natural rutile were <20% in the pH region of 4–11. The highest recovery (13.65%) of natural rutile was obtained at pH 8. Under this pH value, OHA molecule is the dominant collector species while OHA⁻ anion also exits in the solution (Meng et al., 2015). It is expected that OHA molecule and OHA⁻ anion may aggregate into molecule-anion complex in the solution and at the rutile surface, which could improve the adsorption density of collector on the rutile surface and could aid in the rutile flotation.

As for the activated rutile, the flotation response exhibited three distinct regions depending on pH values. In region 1, from pH 4 to 6.5, the recovery increased notably as the increase in pH. In region 2 (6.5≤pH≤10), rutile could be efficiently floated by OHA, and the rutile recoveries reached a relatively stable value (approximately 83%) in this pH region. In this pH region, rutile surface was negatively

charged, favoring the adsorption of positively charged lead species onto the rutile surface (Wang et al., 2016; Zou et al., 2019).

However, as the pH increased to 11 (region 3), the rutile recovery decreased sharply compared with that at pH 10. $Pb(OH)_2$ is the major lead species at pH 11. It seems that $Pb(OH)_2$ species in the solution could not assist in the flotation of rutile.

These results indicated that lead species could remarkably enhance the rutile flotation with OHA in a neutral or weakly basic solution. In fact, neutral pH is more suitable because pH modifiers are unnecessary at a neutral pH.
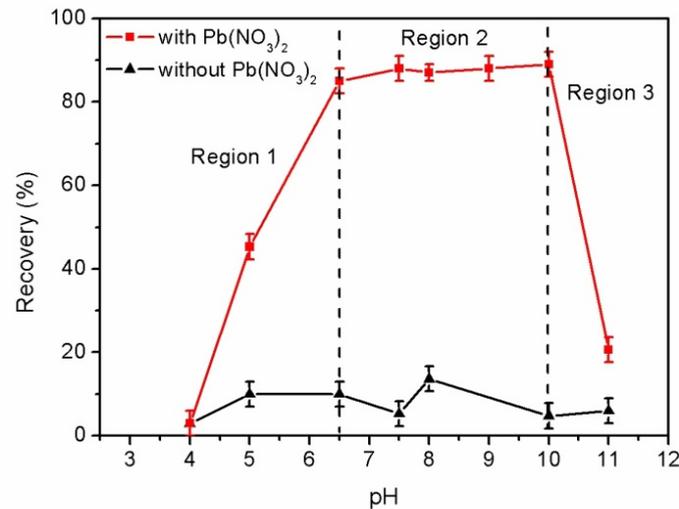

Fig. 2. Effect of pH on the flotation of natural and Pb-activated rutile by using OHA as a collector. The concentrations of OHA and of $Pb(NO_3)_2$ are both 1×10^{-4} mol/dm^3
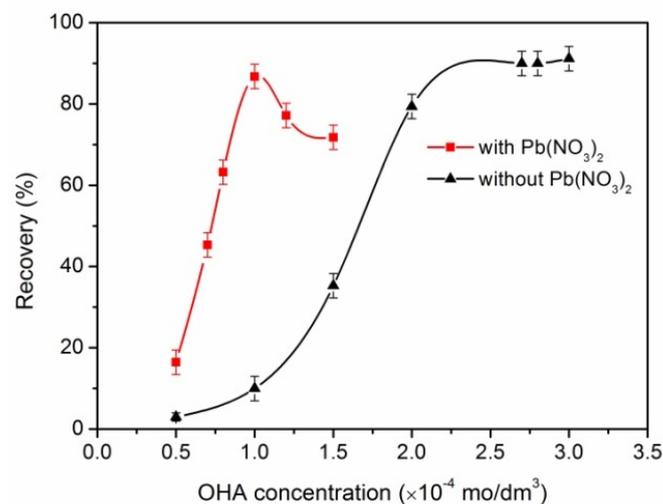

Fig. 3. Flotation results of natural and Pb-activated (1×10^{-4} mol/dm^3 of $Pb(NO_3)_2$) rutile samples as a function of OHA concentration at pH 6.5

Fig. 3 reports the flotation responses of natural and Pb-activated rutile to the OHA concentration at pH 6.5. The $Pb(NO_3)_2$ concentration for the rutile activation was 1×10^{-4} mol/dm^3. For the natural rutile, over 80% of recovery could be achieved only when the OHA concentration was $\geq 2\times10^{-4}$ mol/dm^3. For the Pb-activated rutile, the recovery has reached nearly 85% with 1×10^{-4} mol/dm^3 of OHA. However, the recovery of natural rutile was nearly 10% at the same OHA concentration. Such results demonstrate again that the activation by $Pb(NO_3)_2$ facilitates the rutile flotation with OHA. As the OHA concentration exceeded 1×10^{-4} mol/dm^3, the rutile recovery decreased slightly. We assumed that the Pb atoms on the rutile surface enhance the adsorption and aggregation of OHA on the rutile surface,

and thus surface micelles (bi-layer structure) of OHA probably occur on the rutile surface leading to a decrease in rutile recovery. The assembly structure of OHA on the Pb-activated or natural rutile surface was not probed in this work and should be studied in future.

In addition, OHA molecule and Pb^{2+} are dominate species in the solution at pH 6.5 (Meng et al., 2015; Zou et al., 2019). Thus, it is expected that the interaction between OHA molecule and Pb^{2+} plays an important role in the activation flotation of rutile. The effects of Pb^{2+} on the adsorption of OHA molecule on the rutile surface were further investigated by the DFT calculations in the following parts.

3.2. OHA adsorption studies

3.2.1. Adsorption of OHA molecule on natural rutile surfaces

The OHA molecule was optimized with the CASTEP code (Fig. 4). The O atoms in OH and C=O groups of OHA are termed as O1 and O2 atoms. The optimized OHA molecule was further placed on water- and OH-covered rutile surfaces to search for possible binding models. Fig. 5a shows the stable structure of OHA molecule on the water-covered rutile surface. In this binding model, one water molecule departed from the rutile surface due to the interaction between OHA molecule and the rutile surface. Moreover, the H atom in the OH group of OHA migrated to the top site of a nearby bridging O atom, forming a new OH group. In this regard, OHA^- anion could bind to a 5f-Ti atom on the water-covered rutile surface via a new Ti–O1 bond. The ΔE_{ads} was −33.15 kJ/mol for such binding model.
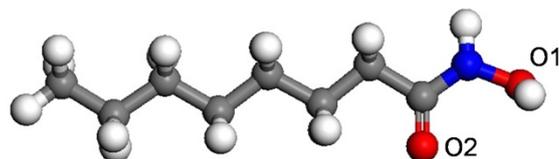

Fig. 4. Optimized OHA molecule (O1: the O atom in OH group; O2: the O atom in CO group)
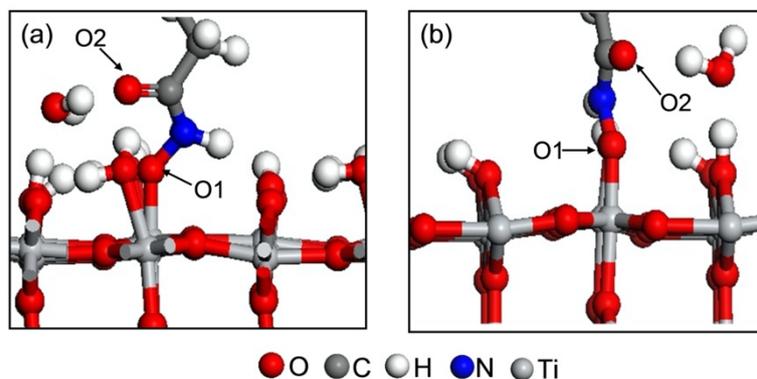

○ O ○ C ○ H ● N ○ Ti

Fig. 5. Stable structures of OHA on (a) water- and (b) OH-covered rutile surfaces

The stable adsorption model of OHA molecule interacting with the OH-covered rutile surface is plotted in Fig. 5b. In this model, one OH group binded with a 5f-Ti atom reacted with the OHA molecule to generate a water molecule, leaving the OHA^- anion to bind with the 5f-Ti atom on the rutile surface and forming a Ti–O1 bond. The ΔE_{ads} of this model was −61.62 kJ/mol.

It was expected that OHA could bind to the Ti atom on the rutile surface to form surface chelate. This binding structure was not observed on the water- or OH-covered rutile surface in this work. Instead, only one oxygen atom of OHA interacted with a Ti atom on the rutile surface. The chemical environment and steric feature of the Ti atoms on the rutile surface may not favor the formation of chelate binding structure.

3.2.2. Adsorption of lead ion on rutile surfaces

Four sites on the water-covered rutile surface may allow the adsorption of Pb^{2+} (Fig. 1a), and the adsorption structures of Pb^{2+} at these sites can be found in (Zou et al., 2019). While, Pb^{2+} could adsorb

at two 4-fold hollow sites on the rutile surface, namely, 4FH4 and 4FH5 sites (Fig. 1b). For the 4FH4 site, the Pb^{2+} ion bonded with three OH groups at this site (Fig. 6a). Differently, four OH groups reacted with Pb^{2+} at the 4FH5 site (Fig. 6b). The ΔE_{ads} values of Pb^{2+} at the 4FH4 and 4FH5 sites were both negative (-1819.29 and -1872.26 kJ/mol), suggesting that Pb^{2+} could readily adsorb onto the OH-covered rutile surfaces.

DFT calculation results demonstrate that it is a thermodynamically favorable process for Pb^{2+} to adsorb onto the water- or OH-covered rutile surface. Further, OHA molecule was inducted into the slab model of Pb-activated rutile surfaces to search the binding models in following parts.
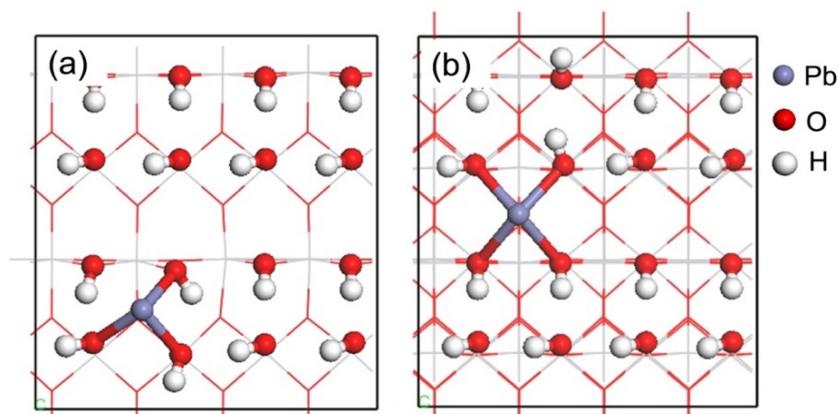

Fig. 6. Adsorption structures of Pb^{2+} at the (a) 4FH4 and (b) 4FH5 sites on the OH-covered rutile surface (bottom atoms are shown in a line style to better view the structure)

3.2.3. Adsorption of OHA on Pb-activated rutile surfaces

OHA molecule could react with the Pb atom at each site on the water-covered rutile surface to generate low-energy configurations. The stable model at each Pb site were illustrated in Fig. 7. In the case of the 4FH1 site, OHA molecule chelate bonded to the Pb_{4fh1} atom on the rutile surface (Fig. 7a). Pb_{4fh1} refers to the Pb atom at the 4FH1 site. For the rest of Pb sites, the adsorption structures of OHA were similar to each other (Figs. 7b-7d). In these binding models, the H from the OH group of OHA molecule dissociated from the molecule to bond with an O atom or an OH group on the rutile surface. Furthermore, OHA^- anion bonded to the Pb atom on the surface, forming a chelation complex.

In addition, the ΔE_{ads} of OHA on the activated water-covered rutile surface was from -256.71 kJ/mol to -136.39 kJ/mol (Table 1), and was lower than that on the natural water-covered rutile surface (−33.15 kJ/mol). These results indicated that the Pb atom on the water-covered rutile surface enhanced the interaction between the OHA and the rutile surface. Thus, the adsorption of OHA on the activated rutile surface was improved, comparing with that on the un-activated surface.

Fig. 8 shows the stable structures of OHA at 4FH4 and 4FH5 sites on the activated OH-covered rutile surface. In the case of 4FH4 site, OHA^- anion was formed, and further reacted the Pb atom generating Pb-OHA chelation complex. Differently, OHA molecule could directly bond with the Pb atom at the 4FH5 site. While, the adsorption energies of OHA at the 4FH4 and 4FH5 sites were -101.53 and -151.79 kJ/mol, more negative than those on the natural OH-covered surface (−61.62 kJ/mol). These results revealed that the adsorption of OHA on the activated OH-covered rutile surface was more stable.

In summary, our DFT results implied that the Pb atoms on the water- and OH-covered rutile surfaces assisted in the adsorption of OHA molecule onto the rutile surface. In this regard, the flotation efficiency of rutile with OHA could be highly improved by the addition of lead ion.

Table 1. Adsorption energies of of OHA at each Pb site on the water-covered rutile surface

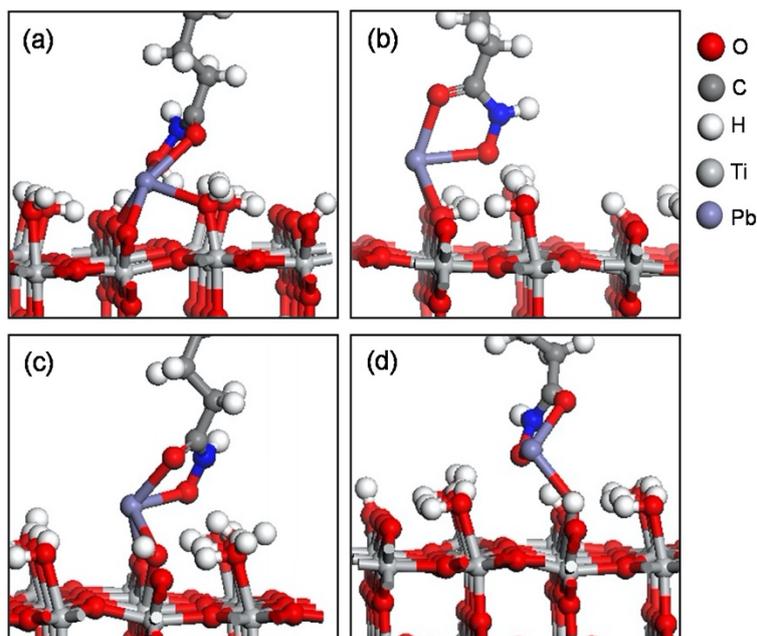| Pb site	4FH2	4FH3	3FH	4FH1
ΔE_{ads} (kJ/mol)	-256.71	-242.23	-178.55	-136.39

Fig. 7. Most stable structures of OHA at Pb sites on the water-covered rutile surface: (a) 4FH1, (b) 4FH2, (c) 4FH3, and (d) 3FH sites
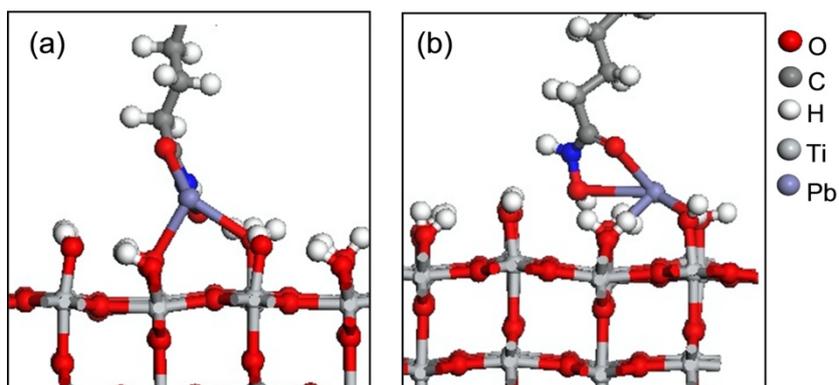

Fig. 8. Stable structures of OHA at Pb sites on the OH-covered rutile surface: (a) 4FH4 and (b) 4FH5 sites

3.3. Electronic structure analysis

The above adsorption structure and energy calculations explain the difference in the affinities of OHA molecule for natural and Pb-activated rutile surfaces. The adsorption of OHA molecule on these rutile surfaces produced new Ti–O and Pb–O bonds. Here, the characters of these new bonds were evaluated on the basis of the electron density difference, bond order and PDOS results to further interpret the effect of Pb^{2+} on OHA adsorption. We only reported the results of the most stable structures of OHA on the water-covered rutile surfaces. The results of the OH-covered surfaces were similar to those on the water-covered rutile surfaces.

Fig. 9a shows the electron density difference slice of the most stable model of OHA on the water-covered rutile without a Pb atom. The charge accumulation and depletion are plotted in blue and red in the figure, respectively. In this binding model, OHA was adsorbed on the rutile surface via a single Ti–O1 bond. Charge accumulation was observed near the O1 atom and in the direction of the Ti–O1 bond. The charge distribution along the Ti–O1 bond is similar to that along the Ti–O_{bulk} bond. The Ti–O_{bulk} bond in rutile is a polarized covalent bond (Murugan et al., 2006). It seems that the Ti–O1 bond also has a certain degree of covalency.

The O1 and O2 atoms of OHA bonded to the Pb atom at the 4FH4 site on the water-covered rutile surface. Charge accumulation was observed among O atoms in the OHA$^-$ anion (Fig. 9b). The variation

in the charge density along the Pb–O1/Pb–O2 bonds was not significant. It is expected that the Pb-O1 and Pb–O2 bonds have a high level of ionicity comparing with the nature of Ti–O1 bond.
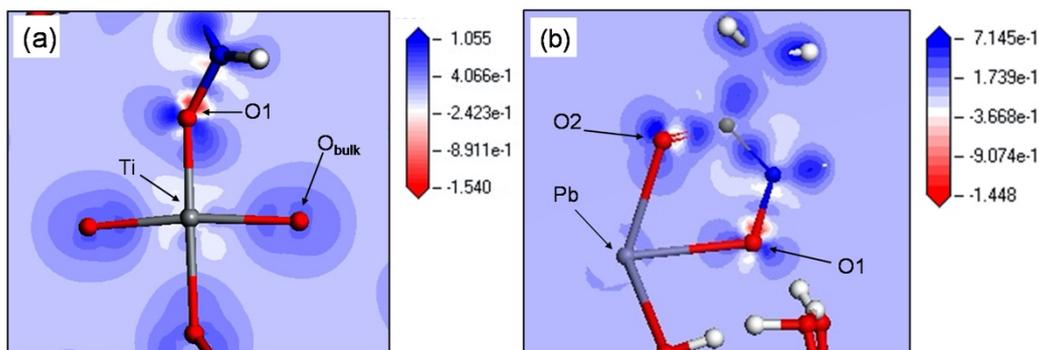

Fig. 9. Electron density difference slices of the most stable binding models of OHA (a) on the water-covered rutile surface and (b) at the 4FH4 site on the activated water-covered surface
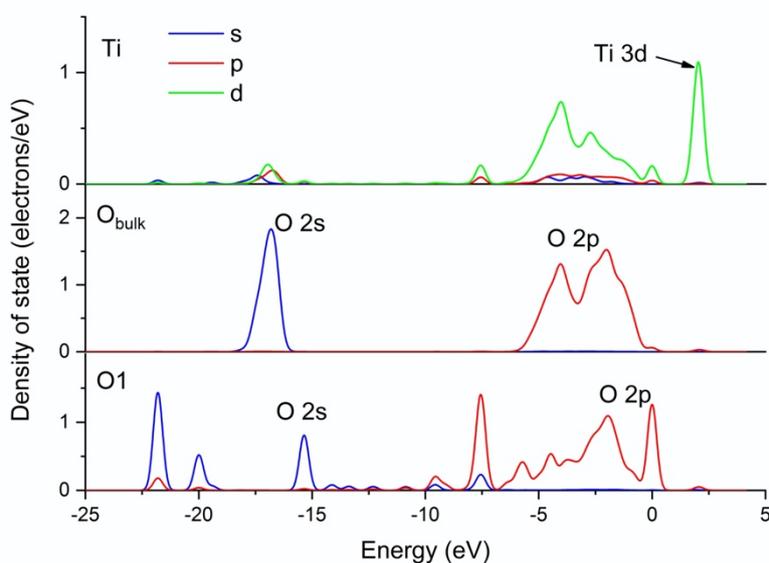

Fig. 10. PDOS diagrams of Ti, O$_{bulk}$ and O1 atoms in the most stable adsorption structure of OHA at the water-covered rutile surface

The covalent nature of above Ti–O1 and Pb–O1/2 bonds could be understood from the bond order and PDOS results, because these results reflect the strength of the covalent bond between interactional atoms. In the case of the adsorption model in Fig. 9a, the bond order of Ti–O$_{bulk}$ was 0.32. For this bond, the Ti 3d and O 2p orbitals overlapped in the valence band near the Fermi level (Fig. 10), accounting for the covalency level in this bond. As for the Ti–O1 bond in Fig. 9a, the bond order was 0.49, which is higher than that of Ti–O$_{bulk}$. This result suggests that the degree of covalency in the Ti–O1 is slightly higher. The covalent nature of Ti–O1 bond was due to the hybridization between the O 2p and Ti 3d orbitals. These two orbitals interacted with each other in the energy level from -8 to 0 eV (Fig. 10), indicating a strong hybridization between them.

However, as for the Pb–O bonds in Fig. 9b, the bond orders of Pb–O1 and Pb–O2 (0. 05 and 0.04) are much less than that of Ti–O1, which supports the above electron density difference conclusion that the covalently level in Pb–O1 or Pb–O2 bond was lower than that of Ti–O1 bond. Moreover, PDOS results showed that the Pb 6p and Pb 6s states did not match well with the O 2p state of O1/O2 in the energy region between -7 to 0 eV (Fig. 11). While the Pb 6s state interacted with the O 2p state in the deeper level in the conduction band (from -11.5 to -7 eV). However, the overlapping area between the Pb 6s and O 2p orbitals was not significant, since the major DOS peaks of these two orbitals were located at different energy levels in the covalence band. The DOS peaks of Pb 6s were mainly located within the energy range from -11.5 to -7 eV. On the contrary, the DOS peaks of O 2p mainly occurred near the

Fermi level (from -7 to 0 eV). In this regard, Pb 6s and O 2p orbitals could not be overlapped efficiently near the Fermi level, resulting in the low covalency degree of Pb–O1/2 bond.
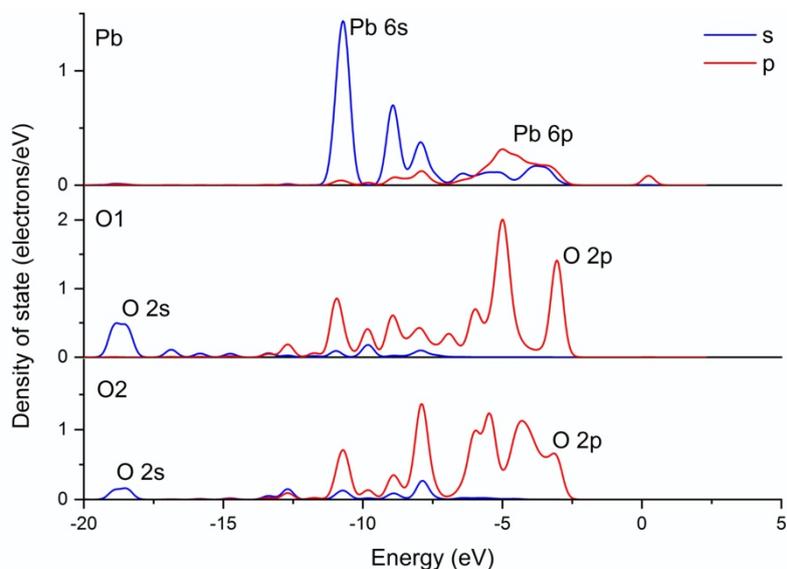

Fig. 11. PDOS diagrams of Pb, O1 and O2 atoms in the adsorption structure of OHA at the 4FH4 site on the activated water-covered surface

It should be stressed that only one O atom of OHA could be involved in the interaction between the OHA and the natural rutile surface, whereas two O atoms of OHA both could bond to the Pb atom on the activated rutile surfaces. Considering that more O atoms of OHA participated in the binding with the surface, the adsorption of OHA on the Pb-activated rutile surfaces was more stable.

A previous study showed that the OHA molecule may chemisorb on the rutile surface (Wang et al., 2016). The binding models calculated in this work provide further evidence for the chemisorption of OHA on the rutile surface. On the other hand, Lin et al. suggested that the OHA molecule could bind with Pb^{2+} on the bastnaesite surface to generate the chelation of Pb-OHA (molecule) based on experimental results (Lin et al., 2020). Our DFT calculation results indicate that OHA molecule and OHA^- anion generated by the dissociation of OHA molecule can both interact with the Pb^{2+} on the rutile surface produce surface chelates. These DFT calculation results extend our knowledge of the interaction between the OHA collector and the Pb^{2+} on the rutile surface.

4. Conclusions

Lead ion could activate the flotation of rutile with OHA in a wide pH region from 6.5 to 10. At pH 6.5, the flotation of rutile was highly enhanced by the addition of 1×10^{-4} mol/dm^3 of $Pb(NO_3)_2$.

OHA molecule dissociated into OHA^- anion on the water- or OH-covered rutile surface. Furthermore, the OHA^- anion could adsorb on the natural surfaces, forming a Ti–O bond.

In the case of Pb-activated rutile surface, OHA molecule may interact with the Pb atom on the surface to generate two Pb–O bonds. While, the dissociation of OHA molecule could happen on the activated rutile surface. As a result, Pb-OHA (anion) chelate complex was produced on the surface. The adsorption of OHA on the activated rutile surface was more stable than that on the natural surface, because the interaction between OHA and the Pb-activated surface generated more chemical bonds. For this reason, the flotation efficiency of rutile with OHA was improved by the addition of lead ion.
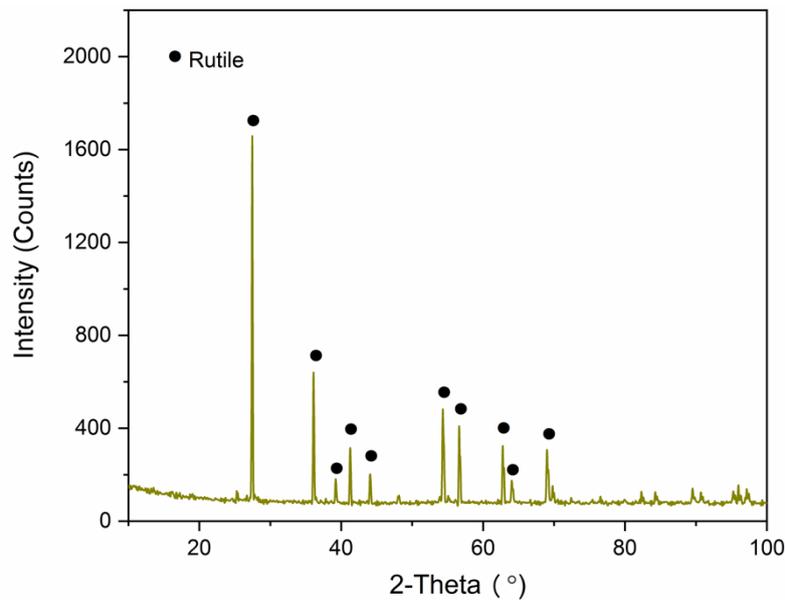
Acknowledgments

Appendix A

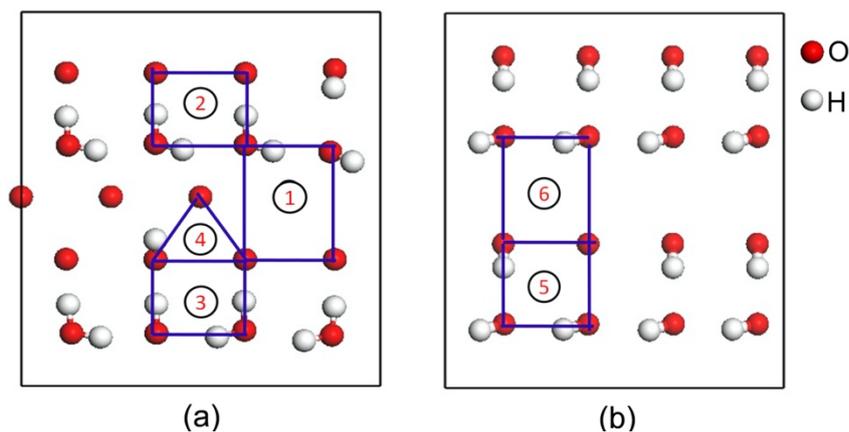Fig. S1. XRD pattern of the rutile sample

Fig. S2. Top view of the adsorption sties for Pb^{2+} on the water- and OH-covered rutile surface: (1) 4FH1 site; (2) 4FH2 site; (3) 4FH3 site; (4) 3FH site; (5) 4FH4 site; (6) 4FH5 site (only the interactional atoms are showed in the figures)

References

BRENNA, B.J., CHEN, J., RUDSHTEYN, B., CHAUDHURI, S., MERCADO, B.Q., BASTISTA, V.S., CRABTREE, R.H., BRUDVIG, G.W., 2016. *Molecular titanium-hydroxamate complexes as models for TiO2 surface binding.* Chem. Commun. 52, 2972-2975.

CHEN, L., WEN, S., XU, G., XIE, H., 2013. *A Novel Process for Titanium Sand by Magnetic Separation and Gravity Concentration.* Miner. Process. Extr. Metall. Rev. 34, 139-150.

FRANCIS, G.P., PAYNE, M.C., 1990. *Finite basis set corrections to total energy pseudopotential calculations.* J. Phys.: Condens. Matter. 2, 4395-4404.

LI, H., MU, S., WENG, X., ZHAO, Y., SONG, S., 2016. *Rutile flotation with Pb2+ ions as activator: Adsorption of Pb2+ at rutile/water interface.* Colloids Surf., A. 506, 431-437.

LIN, Y., CHEN, C., WANG, W., JIANG, Y., CAO, X., 2020. *Beneficial effects and mechanism of lead ions for bastnaesite flotation with octyl hydroxamic acid collector.* Miner. Eng. 148, 106119.

LIU, Q., PENG, Y., 1999. *The development of a composite collector for the flotation of rutile.* Miner. Eng. 12, 1419-1430.

LU, X., ZHANG, H.P., LENG, Y., FANG, L., QU, S., FENG, B., WENG, J., HUANG, N., 2010. *The effects of hydroxyl groups on Ca adsorption on rutile surfaces: a first-principles study.* J Mater Sci Mater Med. 21, 1-10.

MENG, Q., FENG, Q., SHI, Q., OU, L., 2015. *Studies on interaction mechanism of fine wolframite with octyl hydroxamic acid.* Miner. Eng. 79, 133-138.

MURUGAN, P., KUMAR, V., KAWAZOE, Y., 2006. *Thickness dependence of the atomic and electronic structures of TiO2 rutile (110) slabs and the effects on the electronic and magnetic properties of supported clusters of Pd and Rh.* Phys. Rev. B. 73, 075401.

PERDEW, J.P., BURKE, K., ERNZERHOF, M., 1996. *Generalized gradient approximation made simple.* Phys. Rev. Lett. 77, 3865.

PERDEW, J.P., ZUNGER, A., 1981. *Self-interaction correction to density-functional approximations for many-electron systems.* Phys. Rev. B. 23, 5048.

PERRON, H., DOMAIN, C., ROQUES, J., DROT, R., SIMONI, E., CATALETTE, H., 2007a. *Optimisation of accurate rutile TiO2 (110), (100), (101) and (001) surface models from periodic DFT calculations.* Theor. Chem. Acc. 117, 565-574.

PERRON, H., VANDENBORRE, J., DOMAIN, C., DROT, R., ROQUES, J., SIMONI, E., EHRHARDT, J.J., CATALETTE, H., 2007b. *Combined investigation of water sorption on TiO2 rutile (1 1 0) single crystal face: XPS vs. periodic DFT.* Surf. Sci. 601, 518-527.

PREDOTA, M., BANDURA, A.V., CUMMINGS, P.T., KUBICKI, J.D., WWSOLOWSKI, D.J., CHIALVO, A.A., MACHESKY, M.L., 2004. *Electric Double Layer at the Rutile (110) Surface. 1. Structure of Surfaces and Interfacial Water from Molecular Dynamics by Use of ab Initio Potentials.* J. Phys. Chem. B. 108, 12049-12060.

PREMARATNE, W.A.P.J., ROWSON, N.A., 2003. *The Processing of Beach Sand from Sri Lanka for the Recovery of Titanium Using Magnetic Separation.* Phys. Sep. Sci. Eng. 12, 13-22.

SEBBARI, K., DOMAIN, C., ROQUES, J., PERRON, H., SIMONI, E., CATALETTE, H., 2011. *Investigation of hydrogen bonds and temperature effects on the water monolayer adsorption on rutile TiO2 (110) by first-principles molecular dynamics simulations.* Surf. Sci. 605, 1275-1280.

SEGALL, M., LINDAN, P.J., PORBERT, M.A., PICKARD, C., HASNIP, P., CLARK, S., PAYNE, M., 2002. *First-principles simulation: ideas, illustrations and the CASTEP code.* J. Phys.: Condens. Matter. 14, 2717.

USGS, 2019. Mineral commodity summaries 2019: U.S. Geological Survey. U.S. Government Publishing Office.

WANG, J., CHENG, H.W., ZHAO, H.B., QIN, W.Q., QIU, G.Z., 2014. *Flotation behavior and mechanism of rutile in presence of sodium oleate.* Chin. J. of Nonferrous Met. 24, 820-825.

WANG, J., CHENG, H.W., ZHAO, H.B., QIN, W.Q., QIIU, G.Z., 2016. *Flotation behavior and mechanism of rutile with nonyl hydroxamic acid.* Rare Met. 35, 1-6.

XIAO, W., CAO, P., LIANG, Q., HUANG, X., LI, K., ZHANG, Y., QIN, W., QIU, G., WANG, J., 2018a. *Adsorption behavior and mechanism of Bi(III) ions on rutile–water interface in the presence of nonyl hydroxamic acid.* T Nonferr. Metal Soc. 28, 348-355.

XIAO, W., CAO, P., LIANG, Q., PENG, H., ZHAO, H., QIN, W., QIU, G., WANG, J., 2017. *The Activation Mechanism of Bi3+ Ions to Rutile Flotation in a Strong Acidic Environment.* Minerals 7, 113.

XIAO, W., FANG, C., WANG, J., LIANG, Q., CAO, P., WANG, X., ZHANG, L., QIU, G., HU, J., 2018b. *The role of EDTA on rutile flotation using Al^{3+} ions as an activator.* Rsc. Advances 8, 4872-4880.

XIAO, W., JIAO, F., ZHAO, H., QIN, W., QIU, G., WANG, J., 2018c. *Adsorption Structure and Mechanism of Styryl Phosphoric Acid at the Rutile–Water Interface.* Minerals 8, 360.

YANG, X., LIU, S., LIU, G., ZHONG, H., 2017. *A DFT study on the structure–reactivity relationship of aliphatic oxime derivatives as copper chelating agents and malachite flotation collectors.* J. Ind. Eng. Chem. 46, 404-415.

YU, X., CAO, Q., ZOU, H., PENG, Q., 2019. *Activation Mechanism of Lead Ions in the Flotation of Rutile Using Amyl Xanthate as a Collector.* Min., Metall., Explor. 1-12.

ZHANG, W., ZHU, Z., CHENG, C.Y., 2011. *A literature review of titanium metallurgical processes.* Hydrometallurgy 108, 177-188.

ZHENG, T., WU, C., CHENG, M., ZHANG, Y., CUMMINGS, P.T., 2016. *Molecular mechanics of the cooperative adsorption of a Pro-Hyp-Gly tripeptide on a hydroxylated rutile TiO2 (110) surface mediated by calcium ions.* Phys. Chem. Chem.Phys. 18, 19757-19764.

ZOU, H., CAO, Q., CHEN, X., LIU, D., 2019. *Adsorption of lead ion on the hydrated rutile (110) surface: a DFT calculation study.* Physicochem. Probl. Miner Process.. 55, 951-959.